Reduction of the glass transition temperature of confined polystyrene nanoparticles in nanoblends

Yahya Rharbi*
Laboratoire de Rheologie, UJF/INPG/CNRS, PB 53, Domaine Universitaire 38041, Grenoble, France
(Received 15 February 2007; published 21 March 2008)

The role of nanoconfinement on the glass transition temperature (T_g) of polymers has been extensively studied in the thin film geometry. This work looks at the T_g of nanoconfined polystyrene (PS) in spherical nanoparticles (27–200 nm), individually dispersed in crosslinked polybuthylmethacrylate matrices. A reduction of T_g compared to the bulk was observed in PS nanospheres via neutron scattering mechanical tests and was found to decrease with decreasing diameter for $D<50$ nm. The general trend of T_g depression in nanospheres was found to be similar to the results on thin film geometry.

DOI: 10.1103/PhysRevE.77.031806 PACS number(s): 61.41.+e, 82.35.Np, 64.70.P−, 61.05.fg

The glass transition (T_g) of nanoconfined polymers has been extensively studied throughout the last decade [1–12]. The majority of this research has focused on thin film geometry and was carried out on supported and free-standing films using various experimental techniques; Brillouin light scattering [2], ellipsometry [3,5], dielectric relaxation [4], x-ray reflectivity [10], and fluorescence [7,8]. Mechanical measurements on nanobubble inflation have also been used to probe T_g in ultrathin films [9]. These reports substantially agreed that the T_g of polystyrene (PS) decreases with decreasing film thickness for $h<50$ nm. They demonstrate the relevance of polymer structure and polymer and/or substrate interactions in confined T_g. Some reports also raised the question of the influence of thin film sample preparation (spin coating) on T_g reduction [13]. This issue could be settled by studying samples prepared by other means.

Although polymers are often found nanoconfined in geometries such as spheres, little effort has been dedicated to the study of their glass transition. This information could be useful in many industrial and environmental applications: blends, copolymers, nanocomposites, colloids, coatings… . One example is a coating free of volatile organic compound (zero-VOC coating), which uses polymer nanoparticles in the film-making process [14,15]. VOCs are used in coatings to lower the particle T_g, which permits the fabrication of crack-free films at room temperature. If the T_g is reduced by decreasing the nanoparticle size, the use of VOCs could be avoided, which would have a positive impact on the environment. Another example is in nanoblends, where hard polymer nanoparticles are used to reinforce soft matrices. Reducing nanoparticle size would be counterproductive in this application if it causes the reduction of their T_g. It is therefore of utmost importance to tune in to the study of nanoconfined glass transition of polymers in spherical geometries.

Recently, one report presented differential scanning calorimetry (DSC) experiments on aqueous colloidal polystyrene nanospheres in water with diameters ranging from 42 nm up to 548 nm [16]. While they found no clear shift in T_g for the smallest particles they investigated (42 nm), they reported a reduction in the heat capacity [$\Delta(C_p)$] as the particle size decreased. These results were not in agreement with the thin film experiments and might infer that the reduction of T_g in spin coated polystyrene thin films is a signature of the processing history. Other studies on blends and copolymers have attributed the deviations of T_g from bulk values of different components to the mixing of polymers in the interfacial zone [17,18]. In these experiments, the distinction between the effects of mixing and the proximity of two polymers on nanoconfined T_g is not evident. It would be interesting to evaluate the effect of proximity on nanoconfined T_g.

This paper describes the influence of the size and the environment of spherical polystyrene (PS) nanoparticles, on their glass transition and their nanomechanical properties. It looks at the properties of polystyrene confined in nanospheres (27 nm to 130 nm) within polybutylmethacrylate (PBMA) matrices. We use a method which combines nanomechanics and small angle neutron scattering (SANS) to measure the reduction of the glass transition of PS nanoparticles and we compare these results to those found on thin film geometry. This study also focuses on the effect of proximity of two polymers on their glass transition.

Polybutylmethacrylate (PBMA) particles (56 nm) and deuterated polystyrene (dPS) particles were prepared using emulsion polymerization, at 70 °C for PBMA and 80 °C for dPS. The polymer concentrations were 10 wt % for the PBMA and 2 wt % for dPS. The PBMA particles were crosslinked at 10% using ethylene glycol dimethylacrylate (EGDMA) during polymerization. The dPS particle size was controlled between 20 and 200 nm by the amount of surfactant sodium dodecyl sulfate (SDS) in the reaction. The molecular weight measured using gas permeation chromatography (GPC) was found to be around 400 kg/mol–600 kg/mol for all the particles investigated here. Particle diameters (D) were measured using dynamic light scattering (Malvern 5000). The bulk glass transition (T_g^{bulk}) measured by differential scanning calorimetry (DSC Perkin-Elmer, DSC7) yielded the following T_g^{bulk} values between 99 and 102 °C:

D (nm)	27.8	29.8	39.4	52.4	91.2	132.6
T_g^{bulk} (°C)	102.2	99.95	99.2	101.9	99.09	99.44

The surfactant and free ions were removed from the dispersions using a mixture of anionic and cationic exchange resins (Dowex, Aldrich). The nanoblends were prepared by mixing dPS and PBMA dispersions to make dPS concentra-

*rharbi@ujf-grenoble.fr

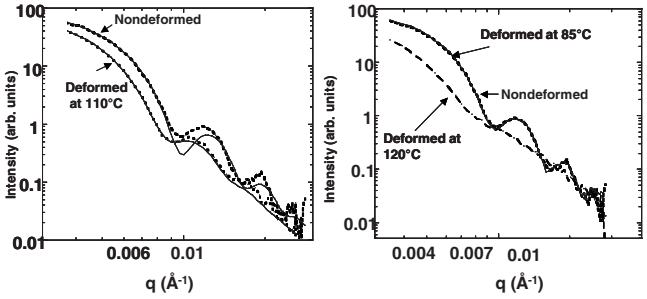

FIG. 1. (a) SANS spectra of polystyrene nanoparticles (2 wt %) with 91.2 nm diameter, in 10% crosslinked PBMA matrices, before deformation and after deformation at 110 °C. The spectra are fitted to the form factor of polydispersed spherical particles. Nondeformed film yields $R=452$ nm and polydispersity index PDI=9%, the deformed film at 110 °C, yields $R=489.9$ nm and PDI=14%. (b) Spectra of the 91.2 nm particle nondeformed, deformed at 85 °C and deformed at 120 °C. The spectra of nondeformed film and the deformed at 85 °C can be completely superimposed.

tions of 0.5, 1, and 2 wt % of the solid PBMA. Solid films were obtained after water evaporation at 45 °C.

The small angle neutron scattering (SANS) experiments were carried out on the PAXY instrument at Orphée, Saclay. The scattered neutrons collected on an *XY* bidimensional multidetector were regrouped according to circular rings to yield spectra of intensities (I) versus the magnitude of the scattering wave vector (q). The range of accessible q values was between 2.3×10^{-3} and 3.4 $Å^{-1}$.

The SANS spectra of films containing up to 2 wt % dPS infer that the dPS nanoparticles are indubitably individually dispersed within the PBMA matrices (Fig. 1). The scattering intensity $I(q)$ is the product of the form factor $P(q)$ and the structure factor $S(q)$ of the dPS particles. Up to a volume fraction of 2%, the structure factor equals 1 and $I(q)=P(q)$. The $I(q)$ intensities were compared to the $P(q)$ of polydispersed hard spheres and the diameter and polydispersity of the particles were calculated from the best fit. These diameters are similar to those from quasielastic light scattering.

Films measuring 5×5 mm in size and 0.5–1 mm thick were compressed in a homemade apparatus in a temperature controlled silicon oil bath by applying a stress of ~4 MPa on the samples for 20 s. The samples were then quenched (for about 20 s) to room temperature in the deformed state. The total experiment lasted around 60 s. During the experiment, the film thickness was reduced to 1/4 of its original size. Because the compressed films were observed with the deformation axis parallel to the neutron beam, the SANS spectra were isotropic. Anisotropy would be seen if the films are visualized with the deformation axis $\perp$ to the neutron beam. The scattering intensity of the deformed film was radially averaged and compared to the spectra prior to deformation. Films containing large PS particles, deformed at temperatures below bulk T_g, yield spectra that are completely superimposable with those before deformation for the whole q range investigated here [Fig. 1(b)]. This infers that (a) although the PBMA matrix deforms by a factor of 400%, the PS nanoparticles remain glassy and do not deform at $T<T_g$; (b) the structure factor $[S(q)]$ of the particles is equal to 1 in the whole range of q values and the deformation of the PBMA matrix does not generate any change in $S(q)$ and consequently on the measured intensity; (c) the idea that cavities develop around hard dPS particles is discarded.

At temperatures above polystyrene T_g, the shape of the SANS spectra of the deformed film evolves with temperature [Fig. 1(b)]. The following three behaviors were observed:

(a) Close to T_g (up to T_g+10), in the rubbery plateau, the spectra shift toward small q values and fit nicely to the form factor of spherical particles. The second and third peaks, exhibiting polydispersity, decrease slightly with increasing temperature.

(b) At 120 °C, the second and third peaks disappear and the intensity continues to shift toward small q values.

(c) For T between 120 and 140 °C, the SANS spectra greatly deviate from the form factor of spherical particles.

To adopt a reliable analysis method three techniques can be used: (1) visual comparison of the shape of the spectra, (2) comparison of the gyration radius, and (3) comparison of the apparent particle diameter measured with the fit to spherical particles.

In the first method (visual comparison), spectra of 90 nm particles, deformed at 85 °C, are completely superimposable with the spectra of the nondeformed films for the whole q range investigated here [Fig. 1(b)]. At temperatures above 105 °C, the spectra shift and the intensity of the second and third peaks start to diminish. On the other hand, the spectra of ~30 nm particles start changing shape well below 100 °C. The shift of the onset temperature for particle deformation is a strong indication that nanomechanical properties of large and small nanoparticles are different.

The second method uses the variation of the gyration radius (R_g) of the particles upon deformation. R_g is estimated from the Guinier plot [Eq. (1)],

$$\ln(I) = \ln(I_0) - \frac{q^2R_g^2}{3}. \tag{1}$$

The Guinier approximation for spherical-shaped particles is valid up to $qR_g\sim2$. The error bar increases above 10% for $qR_g>2$. The situation is more complicated for polymers or elongated fibers where the limit $qR_g<1$ should be respected. By assuming dPS nanoparticles to deform at a constant volume, one can imagine that they flatten with λ in the compression direction and expand with $\lambda^{1/2}$ in the two other axes. The ratio R_g/R_g^0 is an estimation of the rate of particle expansion in the direction perpendicular to the compression and the rate of deformation is calculated as $\lambda(R_g)=(R_g/R_g^0)^2$.

The third method of analysis consists in fitting the SANS intensity to the form factor of spherical particles. The form factor $P(q)$ of the deformed particle is

$$P(q) = I\int \rho(r)e^{-i\vec{q}\cdot\vec{r}}d\vec{r}I^2$$

with

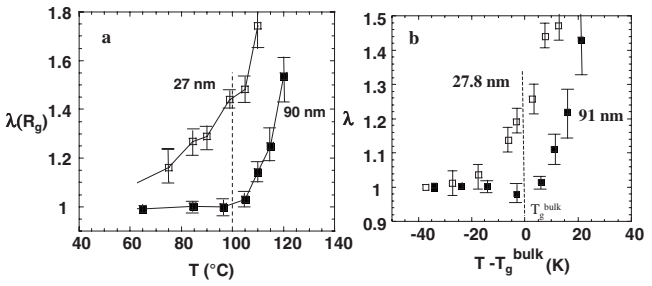

FIG. 2. (a) Deformation rate $[\lambda(R_g)]$ vs temperature for 27 nm and 90 nm dPS nanoparticles in 10% crosslinked PBMA matrix. $\lambda(R_g)$ is calculated using the gyration radius of the particle. (b) λ vs $(T-T_g^{\text{bulk}})$ for 27.8 nm and 91.2 nm dPS nanoparticles in crosslinked PBMA matrix. λ is calculated using the apparent particle diameter from the fit to the form factor of a spherical particle.

$$\frac{x^2}{\lambda}+\frac{y^2}{\lambda}+\lambda^2 z^2 \le R_0^2, \tag{2}$$

$\rho(r)=1$, and 0 otherwise.

If the z axis is the compression direction, parameter q could be rewritten as $q_x'=q_x/\lambda^{1/2}$, $q_y'=q_y/\lambda^{1/2}$, and $q_z'=q_z\lambda$ to give $P(qx,qy,qz)$ of

$$P(q_x,q_y,q_z)=9v_p^2\left(\frac{\sin(q'R_0)-q'R_0\cos(q'R_0)}{(q'R_0)^3}\right)^2, \tag{3}$$

where $q'=(q_x^2/\lambda+q_y^2/\lambda+q_z^2\lambda^2)^{1/2}$. For q perpendicular to the compression direction $q'=(q_x^2+q_x^2)^{1/2}/\lambda^{1/2}=q/\lambda^{1/2}$,

$$P(q)=9v_p^2\left(\frac{\sin(q\lambda^{1/2}R_0)-q\lambda^{1/2}R_0\cos(q\lambda^{1/2}R_0)}{(q\lambda^{1/2}R_0)^3}\right)^2. \tag{4}$$

The $P(q)$ of the deformed spherical particles, with the deformation axis parallel to the neutron beam is equal to $P(q)$ of a spherical particle with diameter $D=D_0\lambda^{1/2}$. The deformation rate of individual particles is calculated as $\lambda=(D/D_0)^2$. A reasonable fit to a spherical particle is possible up to a temperature of 115 °C. Above this temperature the fit to the spherical particles deteriorates and above 120 °C the spectra do not fit to a model of spherical particles.

Figure 2(a) exhibits the deformation rate $\lambda(R_g)$ calculated from the radius of gyration vs temperature for two series of particles, large ~90 nm and small ~27 nm dPS nanoparticles, within 10% crosslinked PBMA matrices. Figure 2(b) shows λ calculated from the ratios of the apparent particle diameter, plotted against (temperature – T_g^{bulk}) for 27.8 and 91 nm particles. The general behavior is the same for both analyses methods used here. The gyration radius can yield a measure of the rate of deformation even if the shape of the particle is no longer ellipsoidal at high temperatures. The deformation rate (λ) for 91.2 nm dPS particles remains constant and equals 1 for temperatures below $T^{\text{onset}}=104$ °C, and increases rapidly above this temperature (Fig. 2). The general tendency of λ vs $[T-T_g^{\text{bulk}}]$ is the same for all particle sizes, however, the whole nanomechanical curve shifts toward low temperatures as the particle diameter decreases. The 27.8 nm dPS particles begin to deform at a lower temperature ($T^{\text{onset}}=91$ °C) than the 91.2 nm particles. This shift

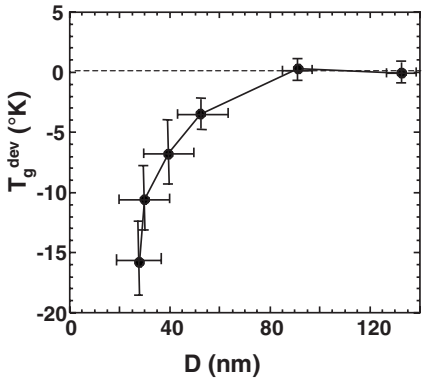

FIG. 3. T_g^{dev} vs dPS particle diameter (D). T_g^{dev} is calculated from the temperature shift of the mechanical curve using the 91 nm or the 130 nm curve as the reference for bulk. Dashed line represents T_g^{bulk}.

is a clear indication that mechanical behavior of small particles is different from that of large ones. Since the mechanical tests were exactly the same for all particle sizes, the shift of the mechanical curve proves, beyond error, that the mechanical behavior deviates from that of the bulk as the particle size decreases below a critical diameter. One explanation for this behavior is that glass transition decreases with decreasing particle diameter. The mechanical curves are superimposable for particle diameters higher than 90 nm, which infers that these large particles exhibit a bulk behavior. The deviation of T_g in small particles compared to the bulk $T_g^{\text{bulk}}(T_g^{\text{dev}}=T_g-T_g^{\text{bulk}})$ is taken as the temperature shift of the nanomechanical curve from the 130 nm particle, which is used here as a reference for bulk. Although the onset temperature of the transition from glassy to rubbery regimes ($T^{\text{onset}}=104$ °C) is close to $T_g^{\text{bulk}}=99.4$ °C for large particles ($D>90$ nm), the T^{onset} is not used here as the nanoconfined glass transition.

Figure 3 shows the dependence of T_g^{dev} on the dPS particle diameter. T_g^{dev} is constant and equal to 0 for particles larger than 50 nm and decreases with decreasing particle size below 50 nm. This result shows a reduction of T_g in polystyrene when nanoconfined in spherical nanoparticles. Note that the error bars for both diameter and T_g^{dev} increase as the particle size decreases. One could imagine that PS and crosslinked PBMA interdiffuse during the compression process and form an interfacial zone of intermediate T_g. Controlled experiments were carried out to estimate the extent of polymer interdiffusion with time. During the compression process (60 s), negligible interdiffusion took place especially in crosslinked PBMA (10%). Therefore, this shows that the reduction of T_g is mostly due to the proximity between dPS and PBMA particles and not to the mixing of the two polymers.

The contribution of Laplace pressure ($P_{\text{Lap}}=4\gamma_{\text{PS-PBMA}}/D$) to particle T_g is negligible; $T_g^{\text{Lap}}=+0.03$ °K for the smallest diameter investigated here. T_g^{Lap} is calculated using $\gamma_{\text{PS-PBMA}}=0.72$ mN/m and $\partial T_g/\partial P_{\text{Lap}}=0.28$ °K/MPa [21]. The Laplace pressure ($P_{\text{Lap}}=0.1$ MPa for 27 nm and 0.02 MPa for 130 nm) could act as a barrier for the deformation of small particles, which could reduce

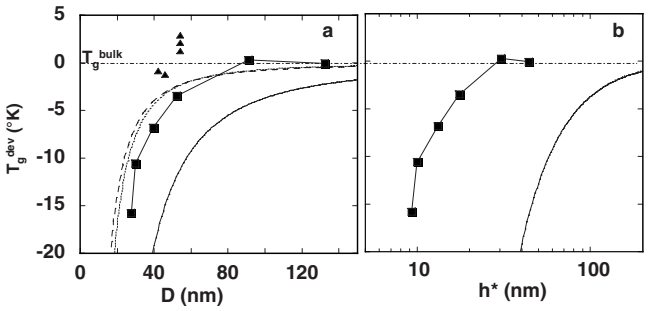

FIG. 4. (a): T_g^{dev} vs dPS particle diameter (D) (■) compared to the DSC results by Sasaki *et al.* on PS nanoparticles (▲) [16], to free-standing PS films [2] (solid line) and to supported PS thin films of Refs. [3] (long dashed line) and [8] (short dashed line). Diameter and film thickness are used interchangeably. (b) T_g^{dev} vs equivalent film thickness h^*, compared to the results on free-standing PS thin films of Ref. [2]. h^* for spherical particles is calculated to yield the same surface to volume ratio as in free-standing thin films ($h^*=D/3$).

the T_g depression as measured from mechanical tests. However, this is not likely to be the case because the applied stress is larger than the Laplace pressure. One can imagine that the applied stress affects the nanoconfined T_g. In the extreme case where the applied stress is fully transmitted to the particle, the nanconfined $T_g$would increase by 1.2 °K due to hydrostatic pressure. The magnitude of the T_g change is independent of particle diameter and therefore the applied stress is less likely to affect the magnitude of T_g reduction.

The authors of Ref. [19] have shown that T_g depression is independent of the molecular weight (MW) distribution in supported PS thin films. Thus the MW polydispersity of polymers made by emulsion polymerization is not likely to play a role in T_g reduction.

The T_g reduction curve in this paper exhibits a similar tendency as those found in free-standing and supported polystyrene thin films with similar MW, when the particle diameter and film thickness are used interchangeably in the x axis ($D=h^*$) [Fig. 4(a)]. This result clearly shows the similarities between thin films and spherical nanoparticles. When T_g^{dev} in spherical particles was fitted to the empirical equation of Ref. [3]

$$T_g^{dev} = -T_g^{bulk}(A/h)^{\alpha}, \tag{5}$$

using $h^*=D$, the α is found to be 2.5 and the characteristic length scale $A=7.7$ nm as opposed to $A=3.2$ nm, $\alpha=1.8$ [3], and $A=4.3$ nm, $\alpha=2$ [8], reported on supported thin films and $A=7.7$ nm, $\alpha=1.8$ in free-standing films with a similar MW [2]. However, the T_g reduction in PS thin films is often related to the total free surface to volume ratio, $S/V=1/h$ for supported films and $2/h$ for free standing films. Spheres exhibit a much larger surface to volume ratio ($S/V=6/D$) than thin films and therefore any comparison between the two situations must be done using the same S/V for both geometries. T_g^{dev} is compared in Fig. 4(b) to the T_g reduction in free-standing films [2] using an equivalent film thickness for spheres $h^*=D/3$ in the x axis instead of the particle diameter. This plot infers that T_g reduction in spherical particles takes place below an equivalent film thickness of $h^*=17$ nm instead of 50 nm in thin films. When T_g^{dev} is fitted with Eq. (5), using the equivalent film thickness $h^*=D/3$, A is found to be 2.6 nm. This might suggest that the characteristic length scale in spherical particles is about three times smaller than that of thin films and therefore, one might conclude that the correlation is geometry dependent.

The quantitative difference between these results and the results on thin films could reside in the difference in their surface mobility and consequently their surface $T_g(T_g^{surf})$. The authors of Ref. [20] estimated a $T_g^{surf}=305$ K for thin films in contact with air. In the present study T_g^{surf} is most likely to be higher than the T_g of crosslinked PBMA (323 K). From the empirical equation that describes the mixing of two polymers ($1/T_g^{surf}=0.5/T_g^{PBMA}+0.5/T_g^{PS}$), the T_g^{surf} was estimated to be 347 K.

Although the two-layer model [20] is a simplified view for describing T_g nanoconfinement, it is explored here to compare thin films and spheres. T_g^{dev} was fitted to an alternative modified two-layer model where the characteristic length scale $\xi(T)$ and T_g^{surf} were the only parameters. The model of Ref. [20] was modified to account for the spherical geometry,

$$T_g^{dev} = [1-(1-2\xi(T)/D)^3](T_g^{surf} - T_g^{bulk}),$$

$$\xi(T) = \xi(T_g^{bulk}) + \alpha(T_g - T)^{\gamma}. \tag{6}$$

When $T_g^{surf}=347$ K, $\xi(T)$ is found to vary between 1.2 and 3.7 nm and scales as $\xi(T)=0.32+0.27(T_g-T)^{0.9}$ as opposed to $\xi(T)=2.2+0.21(T_g-T)^{0.9}$ in the free standing films [where $\xi(T)$ varies between 2.2 and 4.7 nm] [20]. The $\xi(T)$ values are found to be similar to those of thin films for $T_g^{surf}=355\pm5$ K.

Ellison and Torkelson [8] showed that there is a gradient in the confined T_g for films thicker than 25 nm. For films thinner than 25 nm, they [8] did not distinguish a mobile layer from the rest of the film and proposed that films of these thicknesses exhibit a single T_g. If this were the case, one would expect to see a single transition in the mechanical curve corresponding to the deformation of the entire 27 nm particle. A more detailed analysis of the 27 nm particle mechanical curve is needed in order to clarify whether the small nanoparticles (27 nm) deform uniformly below bulk T_g or whether it is just the corona that deforms below bulk T_g followed by the deformation of the core above.

Sasaki *et al.* have carried out DSC experiments on PS particles from 42 nm to 548 nm and did not see a clear shift of T_g for the 42 nm particles, but rather a reduction of the $\Delta(C_p)$ with decreasing particle diameter [16]. The results of Ref. [16] are found to be close to our results [Fig. 3(a)], despite the different environments in the two experiments: crosslinked PBMA in our case and water in the experiment of Ref. [16]. They attributed the reduction of $\Delta(C_p)$ to an enhanced surface mobility and estimated the mobile layer thickness to be 3.8 nm. If this value is used in the fit of our

results to Eq. (6), T_g^{surf} is found to be 356 ± 7 K. The surface mobility of PS nanoparticles in contact with water is expected to be higher than when in contact with PBMA. However this is not the case. One possible explanation is that PS end groups at the particle surface bear anionic charges in aqueous medium, which induce strong repulsions between them and therefore might slow down surface mobility in water.

This paper shows the first direct comparison between confinement in thin film geometry and spherical nanoparticles. A shift from bulk $T_g(T_g^{\mathrm{dev}})$ in spherical nanoparticles dispersed in nanoblends was measured. The T_g^{dev} decreases with decreasing particle diameters below $D=50$ nm. Some reports questioned the role of spin coating in T_g reduction of thin films [13]. Although PS nanoparticles and thin films are prepared via different processing methods (emulsion polymerization for spheres and spin coating for thin films), the general trend of T_g reduction is the same in the two situations.

The French neutron facility at the CEA Saclay, and the Laboratoire Léon Brillouin are gratefully acknowledged for the use of the neutron equipment. We thank Dr. F. Boué for stimulating discussions and N. Bassou, A. Benhalima, and N. Giroud for their help with these experiments.

[1] G. Reiter, Europhys. Lett. **23**, 579 (1993).
[2] J. A. Forrest, K. Dalnoki-Veress, J. R. Stevens, and J. R. Dutcher, Phys. Rev. Lett. **77**, 2002 (1996).
[3] J. L. Keddie, R. A. L. Jones, and R. A. Cory, Europhys. Lett. **27**, 59 (1994).
[4] K. Fukao and Y. Miyamoto, Phys. Rev. E **61**, 1743 (2000).
[5] S. Kawana and R. A. L. Jones, Phys. Rev. E **63**, 021501 (2001).
[6] G. B. DeMaggio, W. E. Frieze, D. W. Gidley, M. Zhu, H. A. Hristov, and A. F. Yee, Phys. Rev. Lett. **78**, 1524 (1997).
[7] C. J. Ellison, S. D. Kim, D. B. Hall, and J. M. Torkelson, Eur. Phys. J. E **8**, 155 (2002).
[8] C. J. Ellison and J. M. Torkelson, Nat. Mater. **2**, 695 (2003).
[9] P. A. O'Connell and G. B. McKenna, Eur. Phys. J. E **20**, 143 (2006).
[10] J. H. van Zanten, W. E. Wallace, and W. L. Wu, Phys. Rev. E **53**, R2053 (1996).
[11] F. Varnik, J. Baschnagel, and K. Binder, Phys. Rev. E **65**, 021507 (2002).
[12] R. A. Riggleman, K. Yoshimoto, J. F. Douglas, and J. J. de-Pablo, Phys. Rev. Lett. **97**, 045502 (2006).
[13] M. Alcoutlabi and G. B. McKeena, J. Phys.: Condens. Matter **17**, 461 (2005).
[14] P. A. Steward, J. Hern, and M. C. Wilkinson, Adv. Colloid Interface Sci. **86**, 195 (2000).
[15] M. S. Tirumkudulu and W. B. Russel, Langmuir **21**, 4938 (2005).
[16] T. Sasaki *et al.*, J. Chem. Phys. **119**, 8730 (2003).
[17] D. Rosati *et al.*, Macromolecules **31**, 4301 (1998).
[18] U. Gaur and B. Wunderlich, Macromolecules **13**, 1618 (1980).
[19] O. K. C. Tsui and H. F. Zhang, Macromolecules **34**, 9139 (2001).
[20] J. Mattsson, J. A. Forrest, and L. Börjesson, Phys. Rev. E **62**, 5187 (2000).
[21] P. Zoller and D. J. Walsh, *Standard Pressure-Volume-Temperature Data forPolymers* (Technomic, Lancaster, PA, 1995), p. 171.